surface was fit (least squares) to the AC surface data points; 2. The bicubic surface was subtracted from the AC surface, resulting in a surface that was assessed by a standard roughness analysis method, R_q (Root Mean Square surface height; See ISO 25178). Finally the OARSI grading reference was obtained from Safranin-O stained sections.

Results: The developed algorithm successfully segmented the AC surface of the μCT volumes (Fig 2). In μCT, the surface of sample 1 appears to be smooth with minor roughness (Fig 2a, black arrows), barely visible in histology. In addition to roughness, fissures (Samples 2-5; Fig 2b-e, yellow arrows; OARSI grade 3.5-4.5), erosion (Samples 3-5; Fig 2c-d, blue arrows; OARSI grade 4-4.5) and mid-zone excavation (Sample 5; Fig 2e, green arrow; OARSI grade 4.5) are visible in both μCT and histology. Surface roughness appeared to be associated with OARSI grade: R_q ranged from 23 μm in 1.5 grade (Sample 1) to 44-90 μm in grade 3.5-4.5. (Samples 2-5).

Conclusions: The proposed μCT technique detects roughness in AC surface even when it is not clearly visible in histology. The technique also reveals AC fissuring and erosion. It appears that quantified roughness is associated with increasing OARSI grade suggesting that μCT has potential to quantify superficial AC morphology. This study is an initial contribution towards a semi-automatic user-independent technique for 3D characterization of the AC surface in contrast enhanced μCT scans. However there is a major limitation: by definition the RMS roughness requires an unambiguous surface, which the biological contour is not. Moreover, degenerated AC surface may be geometrically complex requiring more advanced techniques than those presented in this study to quantify roughness and identify both fissures and excavation.

By visually inspecting the μCT surface images, it is evident that sampling a 2D section at a random location or along a random alignment could potentially alter the histopathological score as determined by conventional histology. The presented μCT approach could mitigate this sampling artifact.

To conclude, we have developed a minimally destructive μCT based in vitro technique to quantify AC surface morphology on a greater superficial AC area than possible using standard histology. A more advanced version of this approach may permit user-independent histopathological evaluation of AC surface morphology.

385
CONTRAST-ENHANCED COMPUTED TOMOGRAPHY FOR THE DETECTION OF FEMOROTIBIAL JOINT DISEASE IN AN EQUINE MODEL

B.B. Nelson [†], C.E. Kawcak [†], L.R. Goodrich [†], N.M. Werpy [‡], A. Valdes-Martinez [†], C.W. McIlwraith [†]. [†] *Colorado State Univ., Fort Collins, CO, USA;* [‡] *Univ. of Florida, Gainesville, FL, USA*

Purpose: To compare the use of computed tomography (CT) and CT arthrography (CTR) to other commonly used diagnostic modalities for the detection of femorotibial joint disease.

Methods: Twenty-five client-owned horses with lameness localized to the femorotibial joint (FTJ) compartment(s) (analogous to the human knee) following a positive response to intra-articular analgesia were included. All FTJ compartments were evaluated with radiographs, ultrasound, CT, CTR, and diagnostic arthroscopy. Following a precontrast CT scan, the contrast medium (Omnipaque-350, GE Healthcare, Oslo, Norway) diluted 1:10 with sterile 0.9% saline was aseptically injected into all 3 stifle joint compartments until resistance was detected on the syringe. The limb was fully flexed and extended to disperse the contrast medium and the postcontrast scan was performed (CTR). Articular structures were evaluated on all modalities and the number of detected lesions on each modality was recorded. The modality where the highest number of lesions was detected provided the reference category for comparisons. The determination of agreement between modalities was made using a McNemar's test. Statistical significance was set at $P<0.05$.

Results: Twenty-five stifles were evaluated in twenty-four horses. The primary lesion was more commonly detected in the medial FTJ compartment (24, 96%) when compared to the lateral FTJ compartment (1, 4%). There were no adverse effects (discomfort, swelling, lameness, or infection) observed following intra-articular contrast injection in any horse. The detection of medial cranial meniscotibial ligament injury was confirmed with arthroscopy and was more commonly detected with CTR (9/12, 75%) than with ultrasonography (3/11, 27.3%). Detection of medial meniscal injury was reliably diagnosed with CTR (8/9, 88.9%). The detection of articular cartilage lesions on the medial femoral condyle confirmed with arthroscopy was detected with CTR in 12/20 (60%) cases resulting in a significant disagreement between modalities for the detection of articular cartilage lesions at this location ($P=0.008$). Four subchondral cystic lesions of the proximal tibia were detected with CT and only one of these lesions was detected with radiographs. There was significant disagreement between the findings of femoral and tibial condyle sclerosis on CT when compared to radiographs ($P=0.002$ and $P=0.0001$, respectively) and lesions were more easily detected with CT. Tearing of the cranial cruciate ligament was detected with CTR in 6 joints and in the caudal cruciate ligament in 7 joints. The presence of contrast medium outlining these ligaments provided sufficient resolution to detect surface abnormalities and intra-ligament tearing (Figure 1). Enthesopathy of the cruciate ligaments was better detected with CT compared to radiographs and there was a significant disagreement between modalities ($P=0.006$ and $P=0.008$, respectively).

Conclusions: The lack of detection of articular cartilage lesions on the medial femoral condyle was likely due to the required positioning of the horse on the CT table and not due to the inability for CTR to be used for the detection of articular cartilage surface abnormalities. Other locations on the medial femoral condyle appeared to have adequate resolution at the articular cartilage surface, but were not a common location of articular cartilage damage in this study. Although the use of MRI is the gold standard method for evaluation of knee injury in humans, the longer scan times limit the number of MRI scans that can be performed in a day and are more expensive compared to CT imaging. Conversely, CT scans are faster (completed in minutes) and have higher spatial resolution compared to MRI. With these limitations of MRI, the use of CT and CTR should be considered as an alternative for the diagnostic evaluation of the knee.

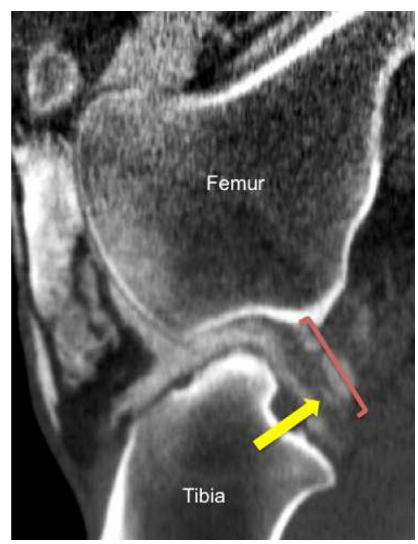

Figure 1. Sagittal reconstruction of a computed tomographic arthrography (CTR) scan of an equine stifle. Cranial (anterior) is to the left and proximal is to the top. The red bracket outlines the caudal cruciate ligament surrounded by hyperattenuating contrast medium. The arrow points to contrast medium within the ligament suggestive of tearing.

386
THE SITE-SPECIFIC ASSOCIATIONS BETWEEN THE MENISCUS CHANGES AND THE OSTEOPHYTE FORMATIONS IN EARLY-STAGE KNEE OSTEOARTHRITIS

S. Hada [†], H. Kaneko [†], R. Sadatsuki [†], L. Liz [†,‡], A. Yusup [†], M. Kinoshita [†], I. Hutami [†], Y. Shimura [§], M. Tsuchiya [§], Y. Saita [†], Y. Takazawa [†], H. Ikeda [†], K. Kaneko [†,‡], M. Ishijima [‖,‡]. [†] *Dept. of Med. for Orthopaedics and Motor Organ, Juntendo Univ. Graduate Sch. of Med., Tokyo, Japan;* [‡] *Sportology Ctr., Juntendo Univ. Graduate Sch. of Med., Tokyo, Japan;* [§] *Juntendo Tokyo Koto Geriatric Med.Ctr, Tokyo, Japan;* [‖] *Juntendo Univ. Sch. of Med., Tokyo, Japan*

Purpose: We recently reported that the degeneration and destruction of femoral articular cartilage and osteophytes showed a greater degree of deterioration than those of the tibial and patellar articular side in early-stage of knee OA using 3TMRI and T2 mapping sequence